Acoustic-domain resonance mode in magnetic closure-domain structures: A probe for domain-shape characteristics and domain-wall transformations

Claudia Hengst,* Manfred Wolf, and Rudolf Schäfer
IFW Dresden, Institute for Metallic Materials, PO 270116, 01171 Dresden, Germany

Ludwig Schultz
IFW Dresden, Institute for Metallic Materials, PO 270116, 01171 Dresden, Germany
and TU Dresden, Department of Mechanical Engineering, Institute for Materials Science, 01062 Dresden, Germany

Jeffrey McCord
Kiel University, Institute for Materials Science, Kaiserstrasse 2, 24143 Kiel, Germany
(Received 4 April 2014; revised manuscript received 22 May 2014; published 13 June 2014)

The magnetic-domain resonance was studied for varying closure-domain structures in $Co_{40}Fe_{40}B_{20}$ thin-film elements. A domain-shape anisotropy model was introduced, by which a significant increase of the acoustic-domain resonance frequency for decreasing domain width is predicted. We show that magnetic flux closure further increases the domain-width effect on the acoustic-domain resonance frequency. Furthermore, the domain resonance frequency is very sensitive to the effective width of the magnetic-domain walls due to dynamic dipolar interaction. The latter is quantified by calculating the dynamic wall width dependent dipolar fields. Domain-wall transitions in external magnetic fields manifest in either smooth or sudden resonance frequency changes, depending on the involved domain-wall types. Quantitative agreement between experimental and modeled data is obtained. Measuring the acoustic-domain resonance in small excitation fields therefore displays a method to analyze domain-wall instabilities and domain-wall interactions.

DOI: 10.1103/PhysRevB.89.214412 PACS number(s): 75.78.Fg, 75.70.Kw, 75.60.Ch

I. INTRODUCTION

Ferromagnetic resonance is widely used as a characterization method for soft magnetic thin films with uniform magnetization as it allows the determination of static magnetic properties, such as the effective magnetic anisotropy field H_a and the saturation magnetization M_s [1]. Both parameters H_a and M_s contribute to the effective magnetic field H_{eff} that acts on the magnetization and therewith determine the ferromagnetic resonance frequency f_r. For a saturated thin-film material with uniaxial anisotropy and confined lateral dimensions, f_r of the uniform resonance mode can be approximated by Kittel's equation [2]:

$$f_r^2 = \left(\frac{\mu_0\gamma}{2\pi}\right)^2 (H_0 + H_a + M_s[N_z - N_y]) \times (H_0 + H_a + M_s[N_x - N_y]), \tag{1}$$

where H_0 is an applied magnetic bias field parallel to the anisotropy field $H_a = 2K_u/\mu_0 M_s$ parallel to y, $\mu_0 = 4\pi \times 10^{-7}\,\text{V s/A m}$ and $\gamma = 1.76 \times 10^{11}\,1/\text{T s}^{-1}$ being the vacuum permeability and the gyromagnetic ratio, respectively. The demagnetizing factors N_x, N_y, and N_z depend on the sample shape, with z being parallel to the film normal. Note, only for the case of a saturated magnetic element with ellipsoidal shape does Eq. (1) give the exact solution due to the homogeneity of the magnetization and the demagnetization field.

In the nonsaturated state a quasihomogeneous magnetization precession can be excited within individual magnetic domains as long as the local effective field inside the domains is homogeneous on the scale of the domain dimensions. For instance, uniform magnetization precession within magnetic domains was observed in 180° domain configurations [3] and closure-domain structures [4,5]. Due to the dipolar coupling of the magnetization of neighboring domains, one can distinguish between two fundamental domain modes, the acoustic and the optic mode. According to the classical understanding of a coupled magnetization precession in two oppositely magnetized domains, no net magnetization component emerges across the domain walls in the case of the acoustic precessional mode (compare Fig. 1). As a consequence the acoustic mode frequency is expected to be independent of the domain width. In contrast, the optic mode frequency is determined by a dynamic dipolar field contribution to H_{eff} which depends on the domain dimensions and which is due to magnetic charges arising at the domain walls. In zero applied magnetic field the optic-domain mode frequency is always higher compared to the acoustic mode frequency due to the additional contribution of dipolar energy.

First studies by Smit and Beljers on stripe and bubble domain structures in films with perpendicular anisotropy revealed an optical-domain mode with a frequency in the gigahertz regime, whereas the acoustic-domain mode frequency was found to reach some hundred megahertz only [6]. For films of high quality factor $Q \gtrsim 1$ the acoustic-domain mode frequencies may reach some gigahertz, depending on Q (see, e.g., Ref. [7–9]). Despite the fact that for low-Q materials ($Q \ll 1$) the acoustic mode frequency is expected to be significantly lower, Queitsch *et al.* [3] observed acoustic-domain resonance frequencies of about 2 GHz in in-plane magnetized domain structures of micrometer-sized

*c.hengst@ifw-dresden.de; http://www.ifw-dresden.de/de/claudia-patschureck

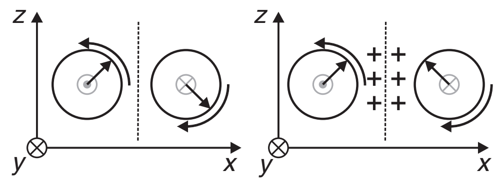

FIG. 1. Cross section of the magnetization precessional cone for two neighboring domains with the equilibrium magnetization (gray) pointing either out of or into the plane of view. In the acoustic-domain mode (left) no dynamic charges are involved as neighboring magnetization vectors precess in phase. The optical-domain mode involves dynamic magnetic poles at the domain boundaries (dashed line).

patterned CoZrTa elements ($Q = 0.0015$). Additionally, it was demonstrated that the domain width severely influences the frequency of the acoustic-domain resonance mode, with $f_{r,\mathrm{ac}}$ increasing from 2.1 to 2.7 GHz when reducing the domain width by a factor of 2. Simultaneously they showed that the cutoff frequency for domain-wall dynamics is on the order of some hundred megahertz. Hence, if the film thickness is small compared to the lateral domain dimensions, the magnetization precession inside the domains occurs in a frequency regime where the domain walls constitute quasirigid transitions between adjacent domains. As a consequence, dynamic charges of opposite sign build up on both sides of a domain wall for an acoustic magnetization precession inside the domains. Based on these findings a model was derived in Ref. [10] in order to take into account the domain dimensions for the calculation of the acoustic-domain mode frequency. Two domains with opposite magnetization direction were approximated by isolated, dipolarly coupled, and magnetically saturated rectangular prisms with a rigid interface in between. According to Ref. [10] the acoustic domain resonance (DR) frequency $f_{r,\mathrm{ac}}$ in thin-film structures ($N_z \rightarrow 1$) and for zero applied field is given by

$$f_{r,\mathrm{ac}} = \frac{\gamma\mu_0}{2\pi}\sqrt{M_s[H_a + (N_x - N_y)M_s + \Lambda_y M_s]}, \quad (2)$$

which is similar to Eq. (1). Here, N_x and N_y represent in-plane ballistic demagnetizing factors [11] according to the dimensions of the basic domains. The dimensionless parameter Λ_y determines the y component of the stray field inside a domain due to the presence of two neighboring domains with $M_y = \pm M_s$. However, in Ref. [10] it was shown that $\Lambda_y \ll (N_x - N_y)$ so that the parameter Λ_y can be neglected in the following.

In contrast to the shape anisotropy of laterally confined magnetic samples with homogeneous magnetization, the domain-shape term $M_s(N_x - N_y)$ is a purely high-frequency contribution. In the static and low-frequency dynamic regime (up to some hundred megahertz), the classical understanding of the acoustic precessional mode still holds: no dynamic charges arise at the domain boundaries as the domain-wall angle adapts to the time-dependent domain magnetization. Beyond the cutoff frequency the permeability of the domain walls nearly vanishes and the quasirigid domain walls get dipolarly charged due to the precessing domain magnetization. In the model presented in Ref. [10] the actual constitution of the magnetic-domain walls is neglected and the calculated demagnetizing field $M_s N_x$ represents the field inside an isolated prism or in a prism with neighbors at distances much larger than the dimensions of the prism (domain-wall width $\gg$ lateral domain dimensions). However, one would expect that the domain-wall constitution, in particular the domain-wall width, tailors the dynamic dipolar interaction and therewith the acoustic mode frequency.

In soft magnetic thin films the magnetization inside a domain wall preferentially rotates within the plane of the film. Depending on parameters such as film thickness, material properties, and applied magnetic field, the width of the domain walls and even the equilibrium domain-wall type may differ, with the symmetric and asymmetric Néel wall, cross-tie wall, and asymmetric Bloch wall being some of the most prominent domain-wall types (see Ref. [12], and references therein). In addition, an external magnetic field may trigger either continuous or spontaneous domain-wall transformations, such as a change of the wall angle or a transition between one domain-wall type and another. The present study investigates the effect of a changing domain-wall configuration on the ferromagnetic DR frequency.

Therefore, we will first extend the domain-shape anisotropy model [10] by considering the effect of magnetic closure domains and particularly the influence of a finite domain-wall width and compare it with experimental results. Thereby we demonstrate that the acoustic DR constitutes a fast and sensitive probe—not only for changes in the domain structure with regard to the domain width but also for domain-wall transitions in applied magnetic fields. Our approach can be used for a rather fast determination of magnetic domain-wall instability fields and a quantitative characterization of magnetic domain-wall interaction in thin films with in-plane magnetic anisotropy. Furthermore, our findings demonstrate the possibility to tune the magnetodynamic response of magnetic thin-film elements by engineering the magnetic-domain structure.

II. EXPERIMENT

Ferromagnetic thin films of amorphous $Co_{40}Fe_{40}B_{20}$ with a thickness of 60 nm and 120 nm were prepared on a glass wafer by means of ultrahigh-vacuum magnetron sputtering. To induce a uniaxial anisotropy an in-plane magnetic field of $H_{\mathrm{dep}} = 20$ kA/m was applied during film deposition. Arrays of stripe ($b \times 9500$ μm, $b = 20, 40$, and 60 μm, $b||H_a$) and square (40×40 $\mu\mathrm{m}^2$) shaped elements were structured using photolithography. The lateral spacing between individual element rows was chosen to be $1.5 \times b$ to minimize effects originating from magnetostatic interaction of neighboring elements. A saturation magnetization of $\mu_0 M_s = 1.48$ T was extracted from out-of-plane magnetization curve measurements of an unpatterned reference film (not shown). In-plane magneto-optical hysteresis measurements along the magnetic hard axis of the reference film (not shown) yield a uniaxial anisotropy field of $H_a = 1.6$ kA/m along the y axis.

After demagnetizing the samples in an alternating external field H_{ini} of decreasing amplitude and a frequency of 50 Hz, closure-domain patterns are observed by magneto-optical Kerr microscopy. By varying the in-plane angle α of the demagnetizing field with respect to the anisotropy axis, the magnetic domain width w was systematically altered from a broad domain state with $H_{\text{ini}}||H_a$ to a narrow domain state with small domain width for $H_{\text{ini}}\perp H_a$.

The dynamic magnetic excitation modes were characterized using a pulsed inductive microwave magnetometer (PIMM) [13]. Therefore the sample was placed upside-down on a coplanar waveguide with a width of 500 μm. The excitation pulse field ($||x$) was oriented perpendicular to the induced magnetic easy axis and in the plane of the film in order to couple to the acoustic DR mode. The DR frequencies are deduced from the peak positions in the amplitude spectra derived using a fast Fourier transformation of the time domain signal. Domain structure analysis after pulse field excitation revealed that no remanent domain structure changes occurred. Hence, the closure structures of varying domain widths represent metastable energy states that are separated by energy barriers high enough to allow for a dynamic excitation with moderate pulse field amplitudes (<0.1 mT) without changing the domain characteristics.

III. EXPERIMENTAL RESULTS

A. Magnetic closure domains

In first experiments, the lateral domain dimensions in patterned stripe elements (thickness 60 nm) were systematically altered by changing the domain width w and the stripe width b in order to verify the domain-shape anisotropy model. Kerr microscopy images of two stripe sections ($b =$ 40 μm) in Fig. 2(a) exemplarily illustrate closure-domain patterns with narrow and broad basic domains, initialized by demagnetization at $\alpha = 0^\circ$, 45°, and 90°, respectively. The experimental change of the acoustic DR frequency with varying domain width w is shown (symbols) for zero applied static magnetic field [Fig. 2(b)].

The acoustic DR frequency increases from 2 up to 3.7 GHz as the domain width decreases by a factor of 5. In addition, a significant dependence of the acoustic DR frequency on the stripe width is expected according to the domain-shape anisotropy model that neglects closure domains (see inset of Fig. 2). However, the experimental $f_{r,\text{ac}}$ turned out to be nearly independent of the stripe width (and therewith the domain length), although the in-plane domain aspect ratio changes up to a factor of 3 ($w =$ constant, $b = 20\ldots60$ m). This can be attributed to the magnetic flux closure at the element edges. Due to the closure domains the demagnetizing field along the y direction nearly vanishes inside the basic domains (i.e., $N_y \cong 0$) and Eq. (2) thus reduces to

$$f_{r,\text{ac}} = \frac{\gamma\mu_0}{2\pi}\sqrt{M_s(H_a + M_s N_x)}. \tag{3}$$

Consequently, for closure-domain configurations the domain-shape anisotropy contribution to the effective field $M_s N_x$ is mainly determined by the domain width and of little account by the domain length (stripe width) and film thickness. The quantitative agreement between the experimental data and the calculated values using Eq. (3) (lines in Fig. 2) demonstrates the validity of the adapted domain-shape approach.

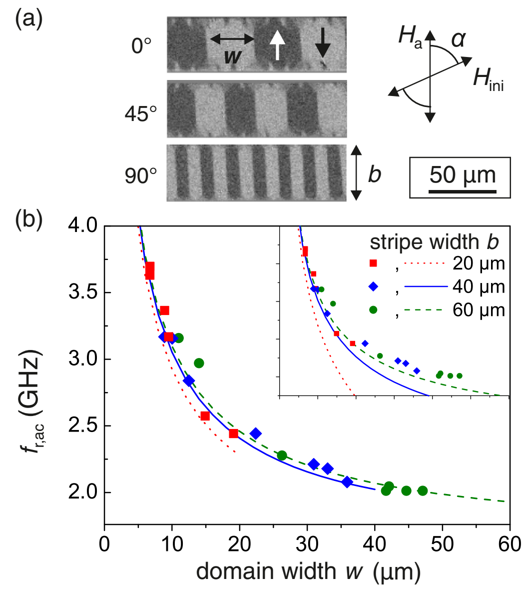

FIG. 2. (Color online) (a) For $b = 40$ μm three characteristic Kerr microscopy images of a narrow, an intermediate, and a broad domain state are shown. (b) The acoustic-domain mode frequency measured for varying stripe width b increases with decreasing domain width w (symbols). Considering the closure domains for the calculation of the domain-shape anisotropy field results in a quantitative agreement between the theoretical (solid lines) and experimental acoustic mode frequencies. Negligence of the magnetic flux closure [Eq. (2); see inset] results in a noticeable overestimation of the influence of the domain lengths.

B. Finite domain-wall width

As the origin of the $f_{r,\text{ac}}(w)$ relation can be ascribed to the dynamic dipolar charging of the domain-wall region, the dipolar field distribution is expected to depend not only on the domain width but also on the width of the 180° domain walls in between the basic domains. For the 60 nm samples discussed in the previous section, Kerr microscopy studies reveal cross-tie walls with an effective wall width of about 3–4 μm [see Kerr image in Fig. 3(a)], which constitutes a substantial fraction of the domain width. By increasing the film thickness to 120 nm the energetically favored wall type was changed from cross-tie to asymmetric Bloch walls, which appear as thin bright or dark vertical lines in the corresponding Kerr image depending on the chirality of the vortex walls. Micromagnetic simulations [14] of a 180° asymmetric Bloch wall and for our set of material properties using OOMMF [15] (not shown) revealed a domain-wall width of $\delta_{\text{bw}} \approx 635$ nm, which corresponds to available literature values [16,17]. Domain resonance was again studied for 60 μm wide stripe elements with varying domain width [symbols in Fig. 3(b)]. In contrast to the results obtained in the previous section the theoretical values calculated according to Eq. (3) based on the ballistic demagnetizing factors $N_x(w)$ of a single prism overestimate the experimental values of $f_{r,\text{ac}}$ significantly.

If the domain-wall width becomes small with respect to the domain width, the dipolar interaction between neighboring domains needs to be taken into account. As illustrated in Fig. 4 any basic domain (represented by a rectangular prism $E_{0,0}$)

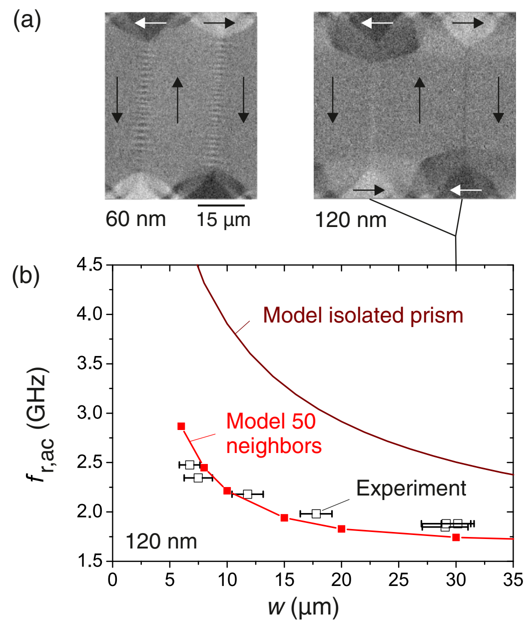

FIG. 3. (Color online) (a) Kerr images of 180° domain walls in stripes of 60 and 120 nm thickness. (b) Comparison of the experimental (data points) and theoretical acoustic DR frequencies of 60 μm wide CoFeB stripes with a thickness of 120 nm. Calculating the domain-shape anisotropy $M_s N_x$ field by using the ballistic demagnetizing factor of an isolated prism by Aharoni [11] overestimates the experimental values. Good agreement is obtained considering the sum of the demagnetizing field and the dipolar field of 50 domains in the neighborhood.

does not only experience the demagnetizing field H_{dx}^{00} due to the magnetic poles generated by its own magnetization $M||x$. It is also subjected to the stray field of all neighboring domains $E_{i,0}$ in a one-dimensional chain of magnetic domains. The strength of this *array field* $H_{dx}^{\sum i0}$ depends predominantly on the domain width w, but also on the domain length and the domain spacing δ_{dw}.

The contribution of a domain $E_{i,0}$ to $H_{\mathrm{dx}}^{\sum i0}$ inside $E_{0,0}$ can be analytically derived using an expression for the dipolar field

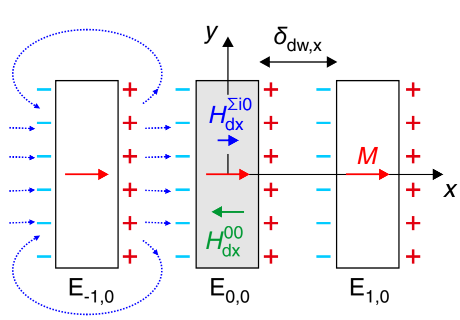

FIG. 4. (Color online) One-dimensional chain of 3 rectangular prisms with $M||x$, according to the hypothetical case of a full opened precessional cone. The element $E_{0,0}$ experiences its own demagnetizing field but also the time-dependent sum of the dynamic stray field of all neighbors which results from dynamic charges at the domain boundaries due to magnetization precession.

given by Aharoni [18]:

$$H_{dx}^{i0} = -\frac{M_s}{4\pi}\frac{\partial}{\partial x}\int_{V_{Ei0}} dV' \times \frac{(x-x')\,m_x(x')}{[(x-x')^2+(y-y')^2+(z-z')^2]^{3/2}}, \quad (4)$$

where $(xyz)'$ refers to an element with $i \neq 0$. With the film thickness t being much smaller than the lateral domain dimensions and the domain spacing, integration with respect to z', y', x' and derivation with respect to x yields the analytical expression for the stray field of an arbitrary domain $i \neq 0$:

$$\begin{aligned} H_{dx}^{i0} &= -\frac{M_s t}{4\pi}\left(\frac{(y-b/2)}{(x-D_i-w/2)\sqrt{(x-D_i-w/2)^2+(y-b/2)^2}}\right. \\ &\quad - \frac{(y-b/2)}{(x-D_i+w/2)\sqrt{(x-D_i+w/2)^2+(y-b/2)^2}} \\ &\quad - \frac{(y+b/2)}{(x-D_i-w/2)\sqrt{(x-D_i-w/2)^2+(y+b/2)^2}} \\ &\quad \left. + \frac{(y+b/2)}{(x-D_i+w/2)\sqrt{(x-D_i+w/2)^2+(y+b/2)^2}}\right), \end{aligned} \quad (5)$$

with $D_i = i(w+\delta_{dw})$. Calculating the sum of all stray fields H_{dx}^{i0} given by Eq. (5) at the position $x = y = 0$ and $H_{dx}^{00} = N_x M_s$ one obtains the domain-shape anisotropy field as a function of the domain width and the domain-wall width. Thereby the contribution of nearest neighbors is most relevant and $H_{dx}^{\sum \mathrm{i0}}$ converges to a maximum value after some tens of micrometers. Considering for example 25 neighbor domains on each side of the domain under consideration yields a good quantitative agreement of the estimated acoustic DR frequency and the experimental values [see Fig. 3(b)]. The results illustrate that the acoustic-domain mode frequency is quite sensitive to varying domain-wall widths due to its influence on the dynamic dipolar interaction between adjacent domains.

C. Domain-wall transitions in transverse magnetic fields

In static magnetic fields transverse to the anisotropy axis the magnetization rotates towards the applied field, which is accompanied by a reduction of the domain-wall angle. At some critical applied field H^* the energetically favored domain-wall type may change and domain-wall transitions can be observed depending on the material properties and the film thickness [19]. For low-anisotropy materials with intermediate film thickness a transition between cross-tie and symmetric Néel walls occurs in transversely applied fields. For larger film thickness a transition between asymmetric Bloch walls and asymmetric Néel walls is expected.

The DR of 40×40 μm^2 CoFeB elements with a film thickness of 60 nm was studied in a superimposed transverse static field that was first increased in amplitude and subsequently reduced back to zero. For the case of a decreasing field amplitude the field- and frequency-dependent permeability is shown in the gray scale map of Fig. 5(a). Dark areas represent a

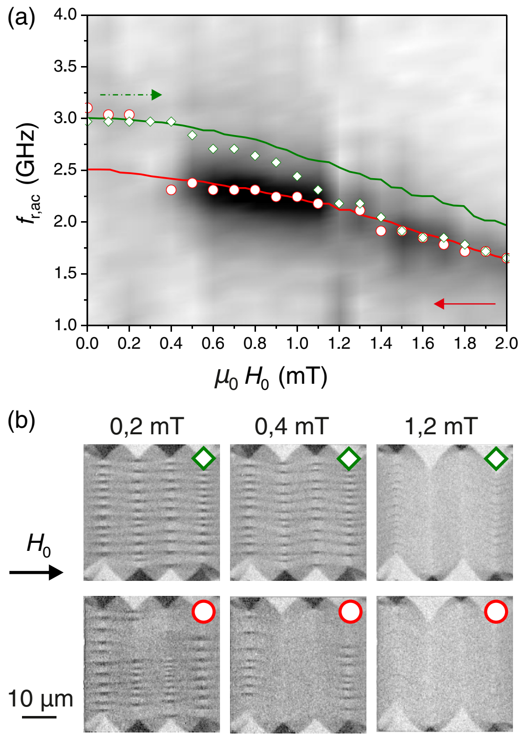

FIG. 5. (Color online) (a) Acoustic DR frequency of $40\times40\ \mu\text{m}^2$ CoFeB elements with a thickness of 60 nm for an increasing (green diamonds) and decreasing (red circles) transverse magnetic field H_0. The underlaid gray scale map reflects the amplitude of the fast Fourier transform of the time-domain signal for the backward branch of the measurement. Dark colors indicate resonance excitation and correspond to the position of the red circles. The red solid line serves for comparison with the theoretical field dependence of $f_{r,\text{ac}}$, assuming that no wall transformation occurs. Wall transformations are the reason why the jump of $f_{r,\text{ac}}$ occurs at different field values for increasing and decreasing field amplitude. (b) Selected Kerr images demonstrate a continuous wall transformation from cross-tie to Néel walls for increasing H_0 and nucleation-dominated backward transformation from symmetrical Néel walls to cross-tie walls.

high permeability and indicate the excitation of DR. For better visibility the position of the permeability maximum is shown by additional data points for both an increasing (diamonds) and decreasing field amplitude (circles).

For $\mu_0 H_0 < 1.2$ mT the measured domain mode frequency depends on whether the field is increased or decreased, resulting in a hysteretic field dependence of the DR frequency. Qualitatively the DR frequency drops with increasing H_0 for both cases due the increasing tilt of the domain magnetization towards the applied field. The solid lines follow the $f_{r,\text{ac}} = f_{r,\text{ac}}(H_0 = 0)\cos\theta$ law known from homogeneously magnetized elements in transversal fields, with θ being the field-dependent angle between the domain magnetization and the anisotropy axis derived from the magnetization loop measurements. Increasing H_0 results in an increasing deviation of the experimentally measured DR frequencies from $f_{r,\text{ac}} = f^0_{r,\text{ac}}\cos\theta$. This is due to the fact that the topology of the cross-tie wall more and more transforms by deformation of the cross-tie legs as the wall angle decreases. At $\mu_0 H_0 = 1.2$ mT the cross ties disappear by movement of the Bloch lines and Bloch line annihilation and the walls are fully transformed into symmetric Néel walls [see Fig. 5(b), top row].

The subsequent reduction of field amplitude leads again to an increase of $f_{r,\text{ac}}$. However, in a field range of 1.2 mT $> \mu_0 H_0 >$ 0.3 mT the measured domain mode frequencies are reduced compared to the increasing field branch. The origin of this irreversibility lies in the self-stabilization of neighboring Néel walls due to interaction of extended Néel wall tails. At 0.3 mT the wall interaction is overcome and the retransformation from Néel into cross-tie domain walls occurs by the nucleation of Bloch lines. The wall transition results in a sudden jump of the domain mode frequency by 0.5 GHz accompanied by a significant decrease of the signal-to-noise ratio. The reduction of permeability upon wall transformation is due to the large fraction of *inactive* domain-wall volume in the presence of cross-tie walls. The reduction of the DR frequency is mainly attributed to the smaller effective wall width ($\approx 2\ \mu$m) for the system of interacting Néel walls.

The asymmetric Bloch wall that displays the equilibrium domain-wall type in 120 nm CoFeB samples for $H_0 = 0$ are

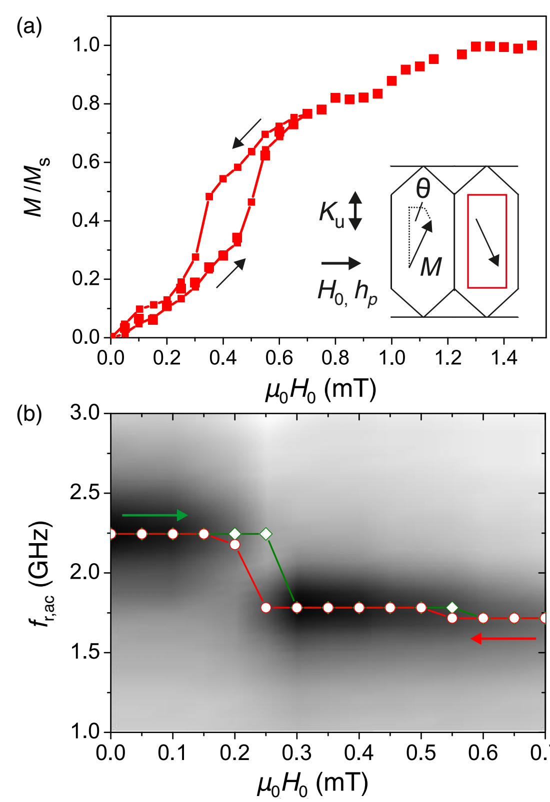

FIG. 6. (Color online) (a) Magnetization curve measured magneto-optically in the center region of a basic domain (see sketch) of a 60 μm wide CoFeB stripe (thickness 120 nm) in a transverse magnetic field. The hysteretic, steplike change in the domain magnetization is associated with the transformation of asymmetric Bloch walls into asymmetric Néel walls. The steplike change is reflected by a hysteretic frequency jump of the acoustic DR (b) for an increasing (green diamonds) and decreasing (red circles) transverse magnetic field H_0. The gray scale intensity map reflects the permeability amplitude spectrum derived from the time-domain signal for the backward branch of the measurement. Dark regions indicate resonance excitation.

expected to undergo a domain-wall transition in transversally applied field as well [19]. The transformation of the domain walls becomes apparent in the magnetization curves measured locally inside the basic domains in an external field applied along the hard axis of magnetization [Fig. 6(a)]. Despite the fact that the domain magnetization progressively rotates towards the field direction a hysteretic jump of the magnetization occurs already at low H_0. This sudden change of the transverse domain magnetization is a consequence of the hysteretic transition from asymmetric Bloch to asymmetric Néel wall and back. No change in domain width takes place. It thereby can be interpreted as an additional rotational contribution $\Delta\theta$ due to the interaction of neighboring Néel wall tails after the wall transition. This argument was experimentally confirmed by quantifying $\Delta\theta$ as a function of domain-wall spacing (to be published separately).

Figure 6(b) shows the permeability map corresponding to the reversal branch of the hysteresis curve. The data points reflect the position of the maximum permeability for increasing (diamonds) and decreasing (circles) transversal field amplitude. Again, a clear jump of the resonance frequency $\Delta f_{r,\mathrm{ac}} \approx 0.5$ GHz occurs at the Bloch-Néel wall transition. The transition field is slightly lower for a decreasing field than for increasing field amplitude. Note, as the transition fields are small the pulse field amplitude adds to the transversal field leading to a slight quantitative mismatch between the static and dynamic transition fields.

IV. SUMMARY

The effects of varying closure-domain structures with different in-plane domain aspect ratio and film thickness on the acoustic-domain resonance was investigated. The domain-shape anisotropy model proposed in Ref. [10] was confirmed by experimental data. In addition to the domain spacing, the magnetic flux closure further increases the domain-width effect on the acoustic DR frequency. In order to model the magnetodynamic response correctly flux closure needs to be taken into account in the domain-shape anisotropy model. Due to dynamic dipolar interaction the acoustic DR is very sensitive not only to domain-shape characteristics but also to the effective width of the exhibited magnetic domain walls. Taking this effect into consideration by calculating the wall-width-dependent dipolar fields, a quantitative agreement between experimental and modeled data is achieved. Magnetic domain-wall transitions manifest in either smooth or sudden resonance frequency changes, depending on the involved domain-wall types. With the presented model the magnetodynamic response of ferromagnetic elements with closure-domain structures can be predicted. This implies that measuring the acoustic DR in small excitation fields represents a potential method to study domain-wall instabilities and domain-wall interactions.

ACKNOWLEDGMENTS

The authors thank K. Kirsch and R. Mattheis (IPHT Jena) for thin-film deposition and I. Mönch (IFW Dresden) for patterning of the films. We gratefully acknowledge fruitful discussions with L. Döring and F. Otto (MPI Leipzig) about the quantitative magnetization profiles of asymmetric domain walls and interacting domain wall systems. C.H. acknowledges financial support that was granted by the Studienstiftung des deutschen Volkes. J.M. acknowledges funding through the Heisenberg Programme of the German Science Foundation (DFG, MC9/9-1) and through Grant No. MC9/10-1.

[1] J. Fassbender and J. McCord, Appl. Phys. Lett. **88**, 252501 (2006).
[2] C. Kittel, Phys. Rev. **73**, 155 (1948).
[3] U. Queitsch, J. McCord, A. Neudert, R. Schäfer, L. Schultz, K. Rott, and H. Brückl, J. Appl. Phys. **100**, 093911 (2006).
[4] K. Perzlmaier, M. Buess, C. H. Back, V. E. Demidov, B. Hillebrands, and S. O. Demokritov, Phys. Rev. Lett. **94**, 057202 (2005).
[5] J. Raabe, C. Quitmann, C. H. Back, F. Nolting, S. Johnson, and C. Buehler, Phys. Rev. Lett. **94**, 217204 (2005).
[6] J. Smit and H. G. Beljers, Phillips Res. Rep. **10**, 113 (1955).
[7] M. Ramesh and P. E. Wigen, J. Magn. Magn. Mater. **74**, 123 (1988).
[8] N. Vukadinovic, J. Ben Youssef, V. Castel, and M. Labrune, Phys. Rev. B **79**, 184405 (2009).
[9] M. Fehndrich and H. Dötsch, Phys. Status Solidi (a) **157**, 127 (1996).
[10] M. Wolf, R. Schäfer, and J. McCord, J. Magn. Magn. Mater. **321**, 2920 (2009).
[11] A. Aharoni, L. Pust, and M. Kief, J. Appl. Phys. **87**, 6564 (2000).
[12] A. Hubert and R. Schäfer, *Magnetic Domains—the Analysis of Magnetic Microstructures*, 3rd ed. (Springer Verlag, Berlin, 1998), pp. 238–271.
[13] A. B. Kos, T. J. Silva, and P. Kabos, Rev. Sci. Instrum. **73**, 3563 (2002).
[14] A 2D simulation was done for a film cross section with a width of 1.2 μm and a thickness of 120 nm, discretized with a mesh of 5 nm $\times$ 5 nm $\times$ 5 nm. A uniaxial anisotropy was set parallel to the cross section with $K_1 = 1.3$ kJ/m^3. The saturation magnetization $\mu_0 M_s = 1.48$ T and the exchange constant of $A = 2.84 \times 10^{-11}$ J/m were chosen to be close to experimental values. An initial two-domain configuration with $M_z = \pm M_s$ was relaxed until $\frac{dm}{dt} = 10^{-9}$.
[15] M. Donahue and D. G. Porter, OOMMF Users's Guide, Version 1.0, Interagency Report NISTIR No. 6376, National Institute of Standards and Technology, Gaithersburg, MD, 1999.
[16] W. Rave and A. Hubert, J. Magn. Magn. Mater. **184**, 179 (1998).
[17] T. Trunk. M. Redjdal, A. Kakay, M. F. Ruane, and F. B. Humphrey, J. Appl. Phys. **89**, 7606 (2001).
[18] A. Aharoni, *Introduction to the Theory of Ferromagnetism*, 2nd ed. (Oxford University Press, Oxford, 2000).
[19] A. Hubert, J. Magn. Magn. Mater. **35**, 249 (1983).